



Article

# Self-Sensing Eco-Earth Composite with Carbon Microfibers for Sustainable Smart Buildings

Hasan Borke Birgin, Antonella D'Alessandro \*, Andrea Meoni and Filippo Ubertini

Department of Civil and Environmental Engineering, University of Perugia, Via Goffredo Duranti 93, 06125 Perugia, Italy

\* Correspondence: antonella.dalessandro@unipg.it; Tel.: +39-0755853910

**Abstract:** This paper proposes a new sustainable earth–cement building composite with multifunctional sensing features and investigates its properties through an experimental campaign. Earth and cement are proportioned as 2/7 in volume, while carbon microfibers are added in various amounts to achieve piezoresistivity, ranging from 0 to 1% with respect to the weight of the binder (i.e., earth + cement). The proposed material couples the construction performance with self-sensing properties in order to monitor the structural performance during the servile life of the building. The use of earth in the partial replacement of cement reduces the environmental footprint of the material while keeping sufficient mechanical properties, at least for applications that do not require a large load-bearing capacity (e.g., for plasters or for low-rise constructions). This paper analyzes the electrical and sensing behavior of cubic and beam samples through electrical and electromechanical tests. The results show that the samples with a filler percentage near the percolation zone, ranged between 0.025 and 0.25%, exhibit the best performance. From the cyclical compressive tests and linear developed models, it could be deduced that the filler content of 0.05% of carbon fibers, with respect to the binder weight, represents the best-performing smart composite for further investigation at higher scales. As demonstrated, the selected mix generated clear strain-sensing electrical signals, reaching gauge factors over 100.

**Keywords:** smart sustainable materials; multifunctional composites; load and strain sensing; piezoresistive self-sensing materials; structural health monitoring; carbon fillers



**Citation:** Birgin, H.B.; D'Alessandro, A.; Meoni, A.; Ubertini, F. Self-Sensing Eco-Earth Composite with Carbon Microfibers for Sustainable Smart Buildings. *J. Compos. Sci.* **2023**, *7*, 63. <https://doi.org/10.3390/jcs7020063>

Academic Editor: Jiadeng Zhu

Received: 31 December 2022

Revised: 21 January 2023

Accepted: 31 January 2023

Published: 6 February 2023



**Copyright:** © 2023 by the authors. Licensee MDPI, Basel, Switzerland. This article is an open access article distributed under the terms and conditions of the Creative Commons Attribution (CC BY) license (<https://creativecommons.org/licenses/by/4.0/>).

## 1. Introduction

Cement and cement-based composite materials are the most used structural materials in modern civil engineering [1] due to their mechanical properties, ease of production, and adaptability to different structural settings [2]. Nevertheless, their impact on the environment is quite high, considering the emissions of CO<sub>2</sub> and other greenhouse gasses, waste production, and high consumption of resources and energy during their production and use [3,4]. Recently, the growing interest in the development of structured approaches to safeguard human health and the environment has led to the diffusion of a multitude of strategies to reduce the impact of the concrete industry [5]. The use of less harmful components and inclusions in the design of mixtures, the optimization of production processes, and the enhancement of strength and durability are among the most frequently used approaches to mitigate the environmental impact of building materials [6,7]. Novel advanced materials, such as fiber-reinforced polymers (FRPs) [8,9] and composites [10,11], which exhibit enhanced properties such as a high strength-to-weight ratio, high durability, and an improved resistance to environmental effects [12,13], are now available to engineers and technicians as effective alternatives to traditional construction materials [14,15]. The use of natural or recycled components in the design of mixtures represents a further exemplification of strategies to reduce the environmental impact of cementitious materials [16,17].

Among the available natural materials, the earth stands forward as a promising alternative or partial substitute of cement. Earth–cement-based composites have been

used for a long time as construction materials and are relatively widespread, especially thanks to their ecological sustainability [18]. They can be produced with relatively low energy consumption, do not require combustion processes, and are compatible with on-site production [19]. Moreover, earth concrete can be easily recycled, thus significantly reducing its ecological footprint [20]. Despite these benefits, the weakness of earth–cement-based composites lies in their mechanical properties. In particular, the tensile strength of cement mixtures containing earth is lower than that of normal concrete, making them even more susceptible to brittle collapse mechanisms [21,22]. The flexural, tensile, and compression strength of the earth concrete can be raised through additives to the binder matrix [23–25]. Some examples of reinforcing earth–cement-based matrices include the dispersion of polypropylene, steel fibers [26], and natural fibers [27,28]. The strengthening fibers can be obtained through recycling, thus further decreasing the environmental footprint of the resulting material [29,30]. Examples include the use of granite cutting residue [31], fibers from recycled tire and steel [32], as well as natural fibers [33]. The dispersion of fibers inside earth concrete can introduce multifunctionalities to the base material, as well as improve its mechanical properties [18,34]. Besides the strength and durability issues, the lack of adequate standards for designing earth-based constructions is another key aspect to be solved in order to achieve feasible practical applications of earth concrete [35]. Possible strategies for the safe application of this construction material are the use of stabilizers [36,37] or the integration of enhanced capabilities [38,39].

Nowadays, multifunctional structural materials are receiving significant interest [40,41]. Among the new functionalities that can be integrated within traditional construction materials through the addition of specific inclusions during their production, the integration of strain-sensing capabilities is a quite attractive strategy to obtain structures and infrastructures capable of self-monitoring their health state in a real-time fashion [34,42]. As demonstrated in the literature, structural materials with strain-sensing capabilities can be effective for the quick assessment of the structural integrity of constructions [43–45]. The literature works also indicate the importance of the optimal choice of the fillers, the design of the sensing material units [46], the tailoring of the electromechanical configuration, and of the post-processing of the signals [47,48] and the investigation of issues and strengths of self-sensing materials in real applications on constructions [49,50]. The analysis of the literature has also pointed out the importance of obtaining a homogeneous dispersion of the fillers within the matrix [51,52]. The authors have recently carried out several experimental campaigns in order to explore the potentials of smart cementitious materials [53,54] and composites [55,56] in applications to structural engineering. In this study, the authors build on their past experience to propose the development of a new sustainable earth–cement-based construction material with strain-monitoring capabilities. Following this approach, the present research explores and discusses key topics for the tailored production and multifunctional applications of innovative eco-friendly smart earth concretes with inclusions of carbon microfibers. The specific scopes can be pointed out in the following steps: (i) the development of a reproducible manufacturing process and (ii) the exploitation of the multifunctionalities of the proposed material using self-sensing properties.

The manuscript is organized as follows: Section 2 introduces the materials, the samples' characteristics, and the devices adopted for the various tests. Section 3 defines the tests carried out on the different types of samples, whose results are presented and discussed in Sections 4 and 5, respectively. Section 6 concludes the paper.

## 2. Materials and Setup

### 2.1. Components and Preparation of Samples

Small cubic samples with 5 cm sidelength and medium-sized beam samples with dimensions of  $4 \times 4 \times 16$  cm were produced as standard samples for mortars. The doping of CMF for the cubes ranged from 0 to 1%, calculated as weight ratios to the earth–cement weight. Two sets were made for the cube samples, the first set containing one test sample out of each mixture with varying CMF doping, and the second set containing five samples

per mixture with CMF doping levels of 0.025, 0.05, and 0.1%. Two additional beam samples were also prepared out of mixtures with CMF doping levels of 0.025, 0.05, and 0.1%.

The dry components of the earth composite of this study were a constitution of excavated earth, aggregates with particle sizes between 0 and 8 mm, and cement. The corresponding mixing proportions calculated per mass were 7/16, 7/16, and 2/16 for the earth, aggregates, and cement, respectively, according to the reference study [36]. The mixing to fabricate the earth composite of this study started with the manual mixing of the earth, aggregates, and cement, followed by the addition and mixing of CMF (Figure 1a). Lastly, the mixing was finished by adding water to the homogeneous mixture of dry components, creating the dough of material, providing sufficient workability for pouring the compound into the molds (Figure 1b). During the molding phase of the mixture, the material was poured into molds and manually compacted to reduce the presence of voids inside the dough. Copper wires were placed at a constant distance, in the central line of the sample, as electrodes for the electrical measurements. The samples were then cured for 28 days under laboratory conditions (Figure 1c).

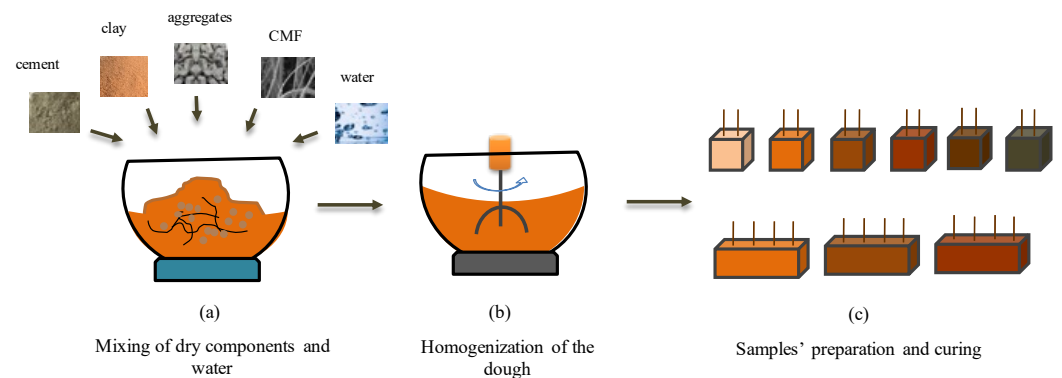


**Figure 1.** The manufacturing steps for smart earth samples: (a) addition of ingredients inside mixing bowl; (b) mixing of the compound until the homogeneity of the composite dough; (c) preparation of small cube and medium-size beam samples from the composite dough, together with the placement of copper electrodes.

Cement is portland cement 42.5R, earth is clay provided by a local regional quarry close to a brick factory in Umbria, Italy. CMF is from SGL Carbon, with the product type SIGRAFIL<sup>®</sup>, having 5  $\mu\text{m}$  diameter and 6 mm fiber length. The electrodes are commercial copper wires with 0.8 mm diameter. A critical aspect of cementitious mixtures with carbon fillers results in the difficult dispersion of the fibers in the matrix for obtaining homogeneity, and in the integrity of the fibers after the preparation procedure. For this purpose, optical microscope and scanning electron microscope inspections were carried out on fragments of hardened material, as shown in Figure 2. Both types of micrographs demonstrate that the carbon fibers appear not damaged and are well dispersed in the composite.

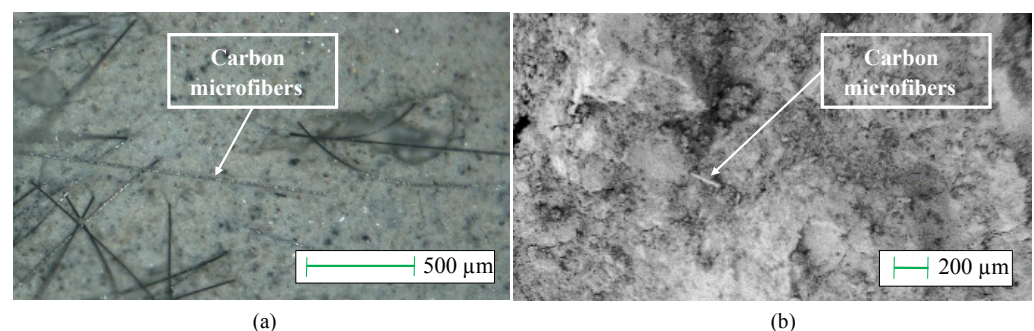


**Figure 2.** (a) Optical microscope and (b) scanning electron microscope inspections on fragments of hardened material.

## 2.2. Experimental Setups

The tests presented in this study were carried out to analyze the electrical resistivity of the developed earth material at different doping levels, as well as the piezoresistive capabilities of the proposed composite for strain sensing. The resistivity of the material samples was obtained through electrical readings taken from unloaded samples. The piezoresistivity was assessed through electromechanical tests performed on the test samples subjected to compressive cyclical loads. The electrical output, which measured the instantaneous electrical resistance of the test sample, was recorded by dedicated hardware capable of reading analog voltage. The recordings were later post-processed to observe the correlation of the test samples' electrical resistance to the induced load and strain. Figure 3 illustrates the experimental setups for resistance readings and electromechanical tests conducted on the different types of samples and setups, i.e., cubes with embedded electrodes placed at a distance of 2 cm and small beams with four aligned electrodes to obtain three subsequent measuring channels.

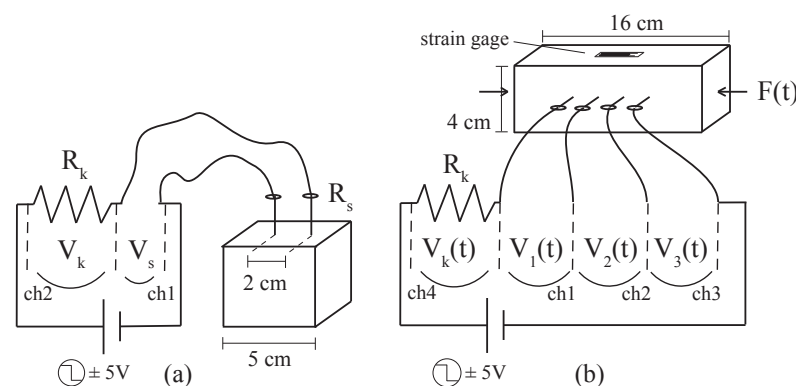


**Figure 3.** Experimental setups for electrical measurements on smart earth samples: (a) cubes for percolation investigation; (b) small-scale beams for electromechanical tests and piezoresistivity analysis.

To interpret the setups shown in Figure 3, the voltage applied to the samples was a 1 Hz biphasic square wave with a 10 V peak-to-peak difference, in order to reduce the polarization effect that may cause a constant positive drift in the resistance–time history and to avoid misleading results. For the data acquisition system during the tests, National Instruments devices and LABVIEW<sup>®</sup> environment were adopted for testing purposes. NI-PXIe 4138 module was used as voltage source apparatus. The analog voltage reader was a 32-channel NI-PXIe 4302 analog-to-digital converter module. The above-listed modules were mounted inside a NI-PXIe 1092 chassis operated in Windows system. The voltage–time history during the tests was sampled with 10 Hz, allowing the selection of 80% of the charge point on the positive phase of the measured square wave. The post-processing of recorded signals was carried out under LABVIEW<sup>®</sup> and MATLAB<sup>®</sup> environments.

For the mechanical equipment of the tests, a software-controlled dynamic compression machine Advantest 9 provided by Controls s.r.l. with a maximum load of 250 kN was used for load application. The induced strains to the material were measured through 2 cm monoaxial strain gauges by KYOWA with an internal resistance of 120 Ohms and a gauge factor of 2.1. The strain gauges attached to the samples were recorded by Advantest9 software simultaneously with the recording of the applied load–time history.

## 3. Electrical Characterization and Sensing Evaluation

The experimental investigation started with the percolation study for the determination of the optimal composite mixture with suitable electrical conductivity. As shown in Figure 3a, the percolation study was conducted by connecting the test sample cubes to an electrical circuit consisting of a biphasic voltage input and a shunt resistor of known value

(i.e.,  $R_k = 100 \text{ k}\Omega$ ) placed in series. Ohm's law (Equation (1)) was employed to calculate the sample resistance–time history.

$$R_s(t) = R_k \frac{V_s(t)}{V_k(t)} \quad (1)$$

where resistance–time history of the sample in ohms ( $R_s(t)$ ) derived from time recordings of voltages spent on the sample and resistor, denoted by  $V_s(t)$  and  $V_k(t)$  (in volts), through data acquisition channels ch1 and ch2.  $R_s$  was determined as the mean value of the readings with a duration of 10 seconds, which corresponded to a set of 10 samples after post-processing of the biphasic signal. Two data sets were investigated for the electrical resistance readings. As previously described, the first one was related to the cubes samples with CMF dopings at weight ratios of 0–0.025–0.050–0.100–0.250–0.500–1.000% of the earth–cement matrix weight. The second set was manufactured for a more detailed inspection of the percolation zone of CMF by containing six samples at the specific CMF weight ratios of 0.025–0.050–0.100% of the earth–cement matrix.

The load-sensing capabilities of the newly produced composite matrix were tested through electromechanical tests. As introduced in previous sections, an electromechanical test assessed and proved the strain-sensing power of the inspected sample by comparing the variation–time history of the electrical resistance with the induced strain–time history ( $\varepsilon$ , positive in compression). The tests for obtaining the strain-sensing performance of the composite material and manufactured sensors were structured following reference [57]. Accordingly, the strains were induced by cyclical triangular compression-applied loads with peak load magnitudes of 0.75–0.75–1.0–1.0 kN with a loading rate of 0.1 kN/s and a precompression load of 0.5 kN. A sample was instrumented during the electromechanical test, and the applied load–time history is plotted in Figure 4a. Referring to the illustration in Figure 3b, the small beams were instrumented by strain gauges, and the electrical readings were taken through three sequential electrode couples located in the central line of the samples ( $V_1$ ,  $V_2$ , and  $V_3$ ). In this way, the three sections between the three electrodes' couples behaved as three resistors connected in series. An additional voltage reading was taken through the shunt resistor ( $V_k$ ) which served as the reference value for measurements from the composite sample. Considering the three monitored segments of the small beams, the related electrical resistances were calculated for all three segments by employing Equation (1) and using  $V_i(t) \forall i \in \{1, 2, 3\}$  instead of  $V_s$ , resulting in  $R_i(t) \forall i \in \{1, 2, 3\}$ . The obtained electrical resistance time histories of the samples correlated with the strain time histories, with respect to the governing equation of the load sensing, which was adopted from the reference study [55] given by Equation (2), under the assumption uniform material properties could be post-processed to calculate the gauge factor  $\lambda_i$ :

$$\lambda_i = -\frac{\Delta R_i}{R_i} = -\frac{\Delta \rho_i}{\rho_i} + (1 + 2\nu) \quad \forall i \in \{1, 2, 3\} \quad (2)$$

where the unitless variable  $\lambda_i$  is the gauge factor of section  $i$ ,  $\rho$  is the piezoresistivity of the material in ohm-meters,  $\nu$  is the Poisson's ratio,  $\varepsilon$  is the induced strain in microstrains, and  $i$  is the segment index of measured electrode pairs. The gauge factor represents the measure of the sensitivity of the smart sensors, obtained with different levels of CMF doping. It is the coefficient of the linear model established between the measured variation in resistance and induced strain. Larger values for the gauge factor are desirable for minimizing the influence of signal noises, therefore improving the sensing quality. As shown by Equation (2), the value of the gauge factor is directly determined by the piezoresistivity of the material ( $\rho$ ) and volumetric deformations of the sample geometry. An optimized composite material design determines a larger contribution of the piezoresistivity than that of the body deformations.

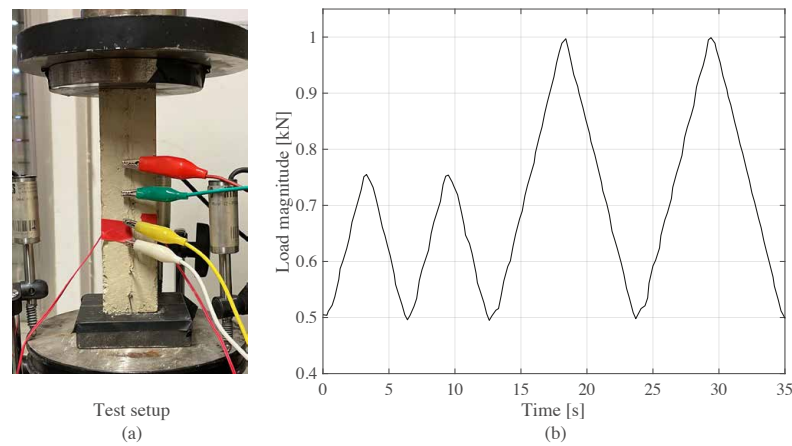


**Figure 4.** Electromechanical tests: (a) experimental setup of a smart earth composite sample, and (b) applied load–time history.

**4. Results**

The percolation curves obtained through the electrical readings revealed the transition of the electrical characteristics of the composite material, showing the percolation threshold which divided the behavior of the material from an electrical insulator to that of one as a conductor. Figure 5 plots the obtained curves out of the experimental readings. Figure 5a depicts the curve of the electrical resistance values, which were obtained by readings conducted on a full sample set. Subsequently, Figure 5b plots the resistance readings of multiple samples of selected CMF doping levels near the percolation threshold. The electrical conductivity transition of the composites started around the CMF doping level of 0.025%, causing a significant decrease in the resistance of the samples until it leveled around 0.25%. After that point, the material’s conductivity increases further with the increasing doping level, with a less sloping trend. The data points plotted in Figure 5a show that the electrical resistance of the samples decreased by an order magnitude of four at the doping level of 1%. The percolation zone of the CMF fillers, according to the given curve in Figure 5a, appears to be around the CMF dopings of 0.025–0.050–0.100%, where it is expected to have an enhanced strain sensitivity due to the piezoresistivity. A further inspection of these levels, considering a higher number of samples, is plotted in Figure 5b. Accordingly, the doping level of 0.050% produced more consistent readings than the other doping levels and exhibited lower noise levels during the tests.

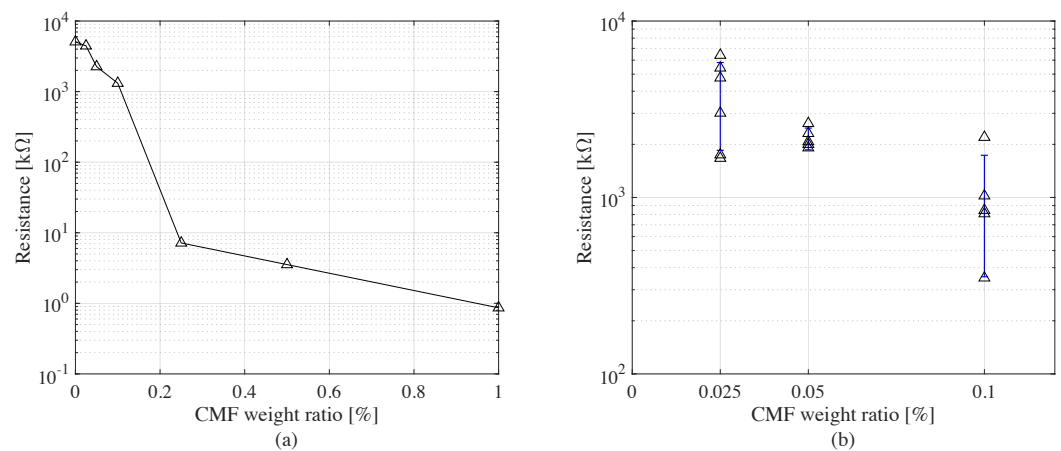


**Figure 5.** Electrical resistance readings of cube samples: (a) electrical resistance values of the sample set ranging 0–1% CMF doping ratios; (b) electrical resistance values of additional samples of critical CMF doping levels of 0.025–0.05–0.1% doping ratios, plotted with mean value and standard deviation.

The linear models of the correlation between the variation in the resistance and induced strain–time histories provide more information about the sensing behavior of the proposed smart earth composites. Figure 6 summarizes the results obtained through the electromechanical tests conducted on the beam samples. In Figure 6, column (a) plots together the recorded time histories of the strain and the fractional change in the sample resistance for all the samples, while column (b) plots the established linear model between the change in the resistance and strain based on the readings. These readings come from the whole body of the sensors. Accordingly, the samples with the 0.025% doping level produced the best performance among all the samples. Especially, the second sample produced a gauge factor of 80, with a very reliable linear model of strain sensing by holding an  $R^2$  value of 0.95. The samples with 0.100% CMF did not provide meaningful results and outputted an excessive noise level. Despite the adequate performance of the first sample of the 0.05% CMF content, the second sample exhibited noise and produced a contradicting performance.

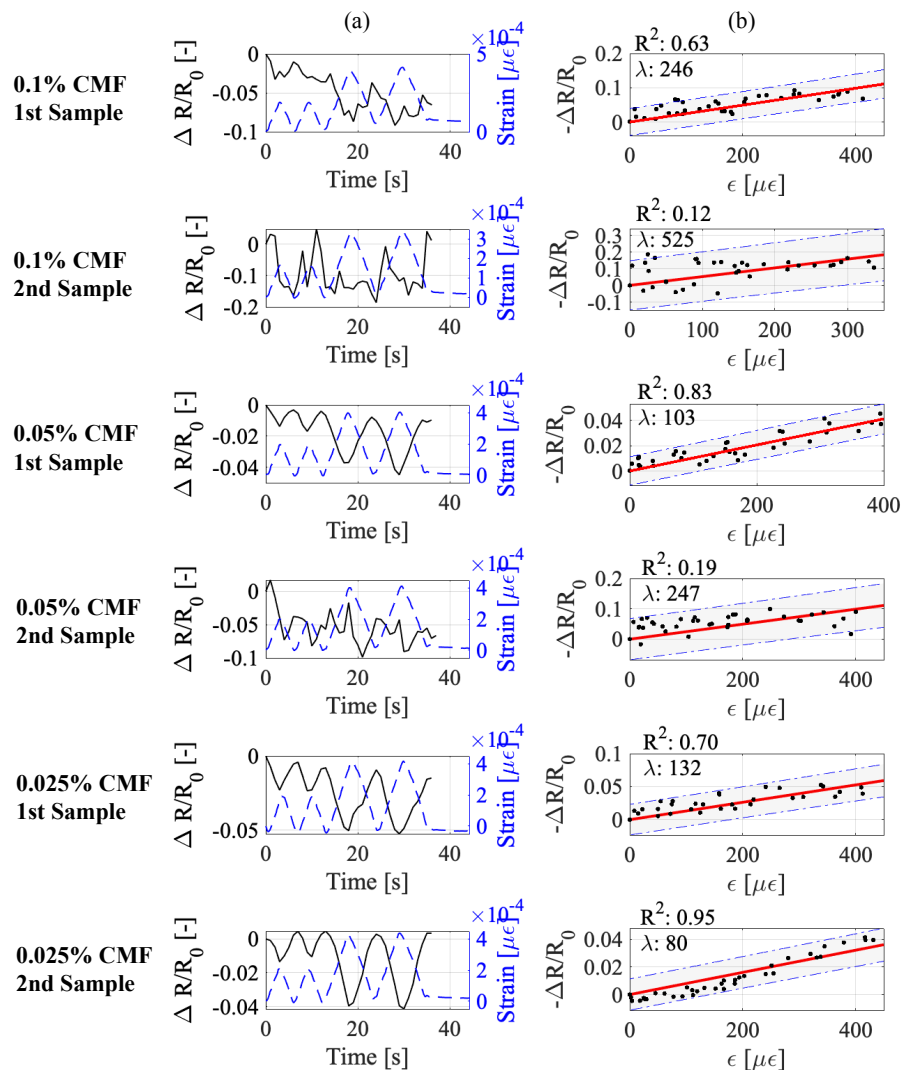


**Figure 6.** The measured signals from the set of beam samples when considering whole sensor volume as the sensor: (a) the time histories of induced strain and the fractional change in sample resistance; (b) the linear models of strain sensing established based on time histories.

The obtained results from the electromechanical tests have been expanded by the addition of multichannel sensing data. Figure 7 plots the fractional change in the resistance data obtained through all the channels indicated by Figure 3b. From the outputs, it was proven that also the second sample made from the 0.05% CMF composite is capable of

sensing the induced strain. The poor performance of part of its volume could be related to the inhomogeneities that likely occur during the production phase of the sample. Even though the samples made from the 0.025% CMF composite performed well considering their full volume, internally they exhibited some irregularities. Unlike the composite material with 0.05%, these irregularities are observed to be consistent for both of the samples. Therefore, the behaviors of the 0.05 and 0.025% samples should have different explanations. Including the findings from Figure 5 into the discussion, it is reasonable to conclude that the composite material with 0.025% of the doping level is affected by the noise and conductivity issues related to poor dispersion of the microfibers. Such issues have played a role in obtaining irregular signals from different volume sections of the 0.025% samples.

The established linear models of the multichannels' strain sensing are shown in Figure 8. In the models, the obtained gauge factors are higher than the ones of the traditional strain sensors. Based on the findings, it can be concluded that the 0.05% composite material has the potential for reliable and reproducible strain sensing. The first sample of this composite material can be selected as the most reliable sensor in the set. However, it is evident that irregularities such as pores or agglomerations exist inside the second sample of this composite, pointing out the importance of the production phase which needs to be carefully controlled. As expected from the above discussion, the strain-sensing performance of the 0.025% CMF material varies through the channels, demonstrating the issues related to under-percolation. Therefore, it is concluded that the optimal CMF content is higher than 0.025% CMF and that the 0.05% CMF content is more promising for further development with the proposed type of material for advanced applications.

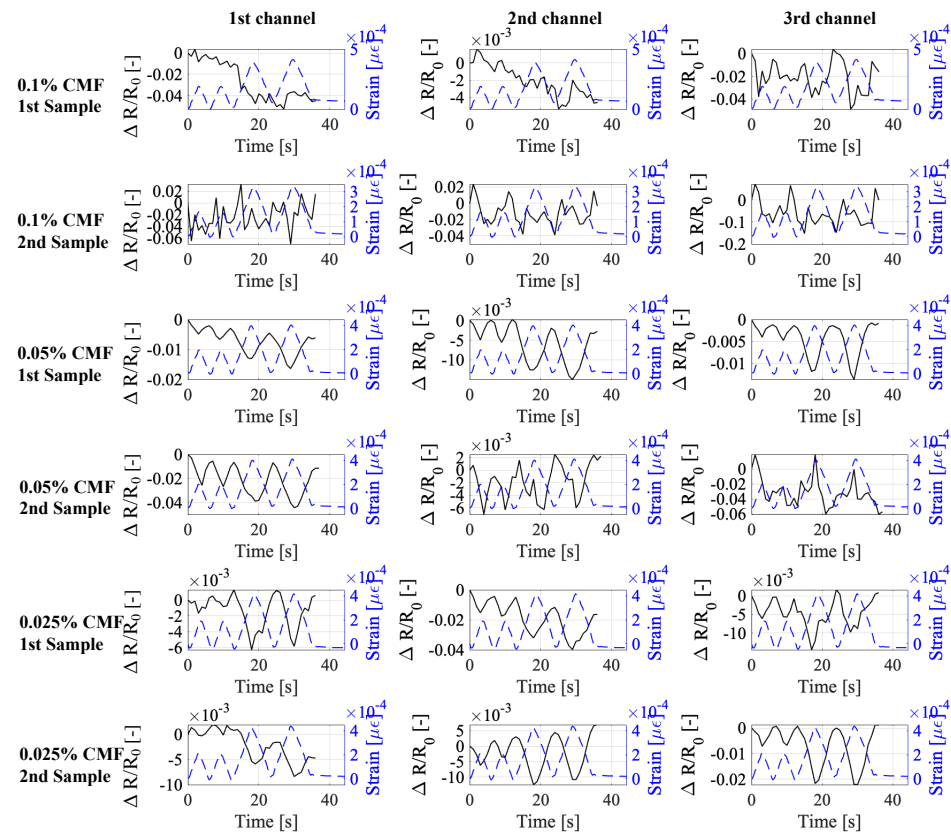


Figure 7. The measured signals from the beam samples; rows contain signals from each sample, and columns contain the data obtained through measurement channels 1, 2, and 3.

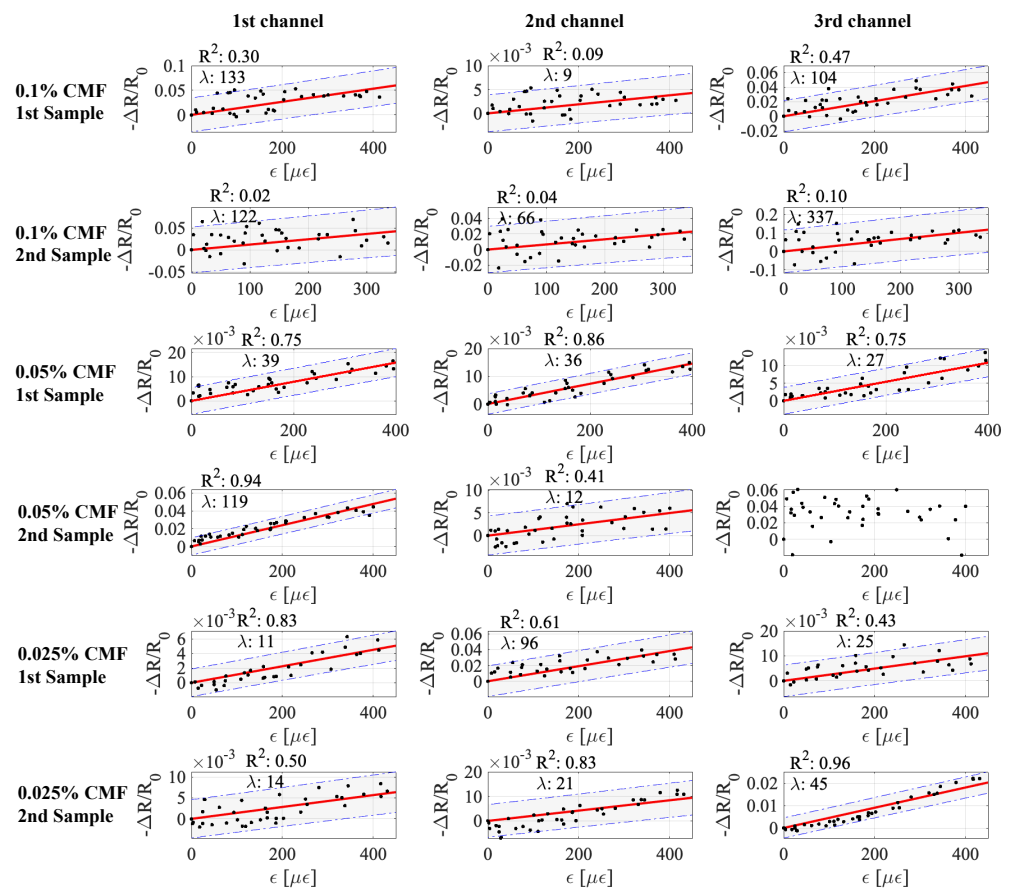


Figure 8. The established linear models of load sensing; rows contain signals from each sample, and columns contain the data obtained through measurement channels 1, 2, and 3.

### 5. Discussion

Multifunctional structural materials have huge application potential. In particular, self-monitoring ones could be particularly useful for enhancing the safety of structures and infrastructures, thus stimulating a lot of ongoing research efforts; however, it is still pivotal to explore different types of materials and investigate their potentialities. This research has proposed and investigated a smart earth–cement composite incorporating carbon microfibers to provide strain-sensing properties. The material has a reduced ecological footprint due to its earth-based matrix and reduced cement content. Different mixtures with varying carbon microfiber contents were studied, particularly considering the following weight percentages of carbon microfibers with respect to the binder matrix weight: 0.025, 0.050, 0.100, 0.250, 0.500, and 1.000%. The characterization tests consisted of electrical resistance readings and highlighted that the critical electrical conductivity state transition zone is between 0.025 and 0.25% of the microfiber content. Further experiments considering additional samples falling within this range pointed out 0.05% as the most promising microfiber content to achieve an effective electrical conductivity.

The second part of the experimental campaign consisted of electromechanical tests to explore the sensing capabilities of the newly produced material. The produced samples are made of mixtures with 0.025, 0.05, and 0.1% microfibers, covering the critical transition zone for the percolation of carbon microfibers. The samples were produced with a tailored design for multichannel readings. The multichannel reading allowed to verify the stability of the 0.05% sample. Although the sample with 0.025% microfibers exhibited a better sensing performance when compared to the 0.05% one when considering the whole sample volume, i.e., in a single-channel reading, the multichannel readings highlighted an improved stability and repeatability of the 0.05% mixture, which is conceivably related to more homogeneous conductive paths within the sample. These findings also agree with

the conclusions made from the percolation curve. It was therefore concluded that despite its good performance, the 0.025% mixture corresponded to the under-percolation of the carbon microfibers, while the 0.05% mixture was closer to the optimum doping amount, and thus more promising for future advances.

Overall, the proposed smart earth–cement material exhibits a very high gauge factor compared to traditional strain sensors, such as resistive strain gauges, thus being suitable for designing sensing networks with reduced instrumentation complexity and costs. This material is also attractive for its sustainable properties related to the limited use of cement in comparison to traditional concrete.

## 6. Conclusions

This paper presents the results of an experimental campaign about the self-sensing capabilities of a novel smart composite composed of an earth–cement matrix doped with carbon microfibers. This composite was investigated for its prospective adoption as a multifunctional construction material with self-monitoring properties. In order to identify an optimal material formulation, conductive fillers were added in relative amounts ranging from 0 to 1% with respect to the weight of the binder. The results of the research show that the optimal mix design to enhance the sensitivity of the material can be identified through electrical and electromechanical tests.

The main remarks of the study are listed as follows. (i) The proposed earth–cement-based smart composite was a building material with sustainable characteristics that was found to possess self-monitoring capabilities. (ii) The electrical resistance readings have revealed that percolation occurred at doping levels from 0.025 to 0.25%. Within this range, the doping percentage of 0.05% of carbon microfibers was pointed out as the one leading to the best linearity and signal quality in the electrical resistance versus strain plots. (iii) Electromechanical tests were also repeated in a multichannel configuration, demonstrating the feasibility of distributed sensing, which is crucial for localizing cracks and internal defects. (iv) The obtained gauge factors were found much larger than those of traditional strain gauges. (v) The varying sizes of the test samples together with the employed manufacturing technique highlighted the scalability of the proposed material for more advanced field applications.

Future steps of the research will concern the sensing capabilities of higher-scale samples, mechanical improvements to the mixture for extensive usability, and the analysis of the different applications where the smart material could be adopted, including full-scale tests.

**Author Contributions:** The following contributions are made by the authors: conceptualization, A.D. and F.U.; methodology, H.B.B., A.D., and A.M.; software, H.B.B.; validation, A.D. and F.U.; resources, F.U.; writing—original draft preparation, H.B.B.; writing—review and editing, A.D. and F.U.; visualization, H.B.B. and A.D.; supervision, A.D. and F.U. All authors have read and agreed to the published version of the manuscript.

**Funding:** The authors acknowledge the support of the Italian Ministry of University and Research (MUR) through Project FISIR 2019: “Eco Earth” (code 00245).

**Institutional Review Board Statement:** Not applicable.

**Informed Consent Statement:** Not applicable.

**Data Availability Statement:** The data presented in this study are available on request from the corresponding author.

**Acknowledgments:** The authors would like to acknowledge FBM Marsciano for providing dry clay.

**Conflicts of Interest:** The authors declare no conflict of interest.

## References

1. Colleparidi, M. *The New Concrete*; Tintoretto: Treviso, Italy, 2010; p. 426. ISBN 9788890377723.
2. Shah, S.P.; Hou, P.; Konsta-Gdoutos, M.S. Nano-modification of cementitious material: Toward a stronger and durable concrete. *J. Sustain.-Cem.-Based Mater.* **2016**, *5*, 1–22. [CrossRef]
3. Van den Heede, P.; De Belie, N. Environmental impact and life cycle assessment (LCA) of traditional and 'green' concretes: Literature review and theoretical calculations. *Cem. Concr. Compos.* **2012**, *34*, 431–442. [CrossRef]
4. Flower, D.; Sanjayan, J. Green house gas emissions due to concrete manufacture. *Int. J. Life Cycle Assess.* **2007**, *12*, 282–288. [CrossRef]
5. Müller, H.S.; Haist, M.; Vogel, M. Assessment of the sustainability potential of concrete and concrete structures considering their environmental impact, performance and lifetime. *Constr. Build. Mater.* **2014**, *67*, 321–337. [CrossRef]
6. Habert, G.; Roussel, N. Study of two concrete mix-design strategies to reach carbon mitigation objectives. *Cem. Concr. Compos.* **2009**, *31*, 397–402. [CrossRef]
7. Cabeza, L.F.; Barreneche, C.; Miró, L.; Morera, J.M.; Bartolí, E.; Inés Fernández, A. Low carbon and low embodied energy materials in buildings: A review. *Renew. Sustain. Energy Rev.* **2013**, *23*, 536–542. [CrossRef]
8. Tucci, F.; Vedernikov, A. Design Criteria for Pultruded Structural Elements. In *Encyclopedia of Materials: Composites*; Brabazon, D., Ed.; Elsevier: Oxford, UK, 2021; pp. 51–68. [CrossRef]
9. Onuralp, O.; Lokman, G.; Emrah, M.; Ceyhan, A.; İlker, K. Effect of the GFRP wrapping on the shear and bending Behavior of RC beams with GFRP encasement. *Steel Compos. Struct.* **2022**, *45*, 193–204.
10. Cassese, P.; Rainieri, C.; Occhiuzzi, A. Applications of Cement-Based Smart Composites to Civil Structural Health Monitoring: A Review. *Appl. Sci.* **2021**, *11*, 8530. [CrossRef]
11. Yu, K.; Lin, M.; Tian, L.; Ding, Y. Long-term stable and sustainable high-strength engineered cementitious composite incorporating limestone powder. *Structures* **2023**, *47*, 530–543. [CrossRef]
12. Vedernikov, A.; Safonov, A.; Tucci, F.; Carlone, P.; Akhatov, I. Analysis of Spring-in Deformation in L-shaped Profiles Pultruded at Different Pulling Speeds: Mathematical Simulation and Experimental Results. Available online: <https://popups.uliege.be/esaform21/index.php?id=4743> (accessed on 30 December 2022).
13. Minchenkov, K.; Vedernikov, A.; Kuzminova, Y.; Gusev, S.; Sulimov, A.; Gulyaev, A.; Kreslavskaya, A.; Prosyanyoy, I.; Xian, G.; Akhatov, I.; et al. Effects of the quality of pre-consolidated materials on the mechanical properties and morphology of thermoplastic pultruded flat laminates. *Compos. Commun.* **2022**, *35*, 101281. [CrossRef]
14. Zhou, P.; Li, C.; Bai, Y.; Dong, S.; Xian, G.; Vedernikov, A.; Akhatov, I.; Safonov, A.; Yue, Q. Durability study on the interlaminar shear behavior of glass-fibre reinforced polypropylene (GFRPP) bars for marine applications. *Constr. Build. Mater.* **2022**, *349*, 128694. [CrossRef]
15. Madenci, E.; Özkılıç, Y.O.; Aksoylu, C.; Safonov, A. The Effects of Eccentric Web Openings on the Compressive Performance of Pultruded GFRP Boxes Wrapped with GFRP and CFRP Sheets. *Polymers* **2022**, *14*, 4567. [CrossRef]
16. Revilla-Cuesta, V.; Faleschini, F.; Pellegrino, C.; Skaf, M.; Ortega-López, V. Simultaneous addition of slag binder, recycled concrete aggregate and sustainable powders to self-compacting concrete: A synergistic mechanical-property approach. *J. Mater. Res. Technol.* **2022**, *18*, 1886–1908. [CrossRef]
17. Leng, Y.; Rui, Y.; Zhonghe, S.; Dingqiang, F.; Jinnan, W.; Yonghuan, Y.; Qiqing, L.; Xiang, H. Development of an environmental Ultra-High Performance Concrete (UHPC) incorporating carbonated recycled coarse aggregate. *Constr. Build. Mater.* **2023**, *362*, 129657. [CrossRef]
18. Van Damme, H.; Houben, H. Earth concrete. Stabilization revisited. *Cem. Concr. Res.* **2018**, *114*, 90–102. [CrossRef]
19. Pacheco-Torgal, F.; Jalali, S. Earth construction: Lessons from the past for future eco-efficient construction. *Constr. Build. Mater.* **2012**, *29*, 512–519. [CrossRef]
20. D'Alessandro, A.; Fabiani, C.; Pisello, A.L.; Ubertini, F.; Materazzi, A.L.; Cotana, F. Innovative concretes for low-carbon constructions: A review. *Int. J.-Low-Carbon Technol.* **2017**, *12*, 289–309. [CrossRef]
21. Fardoun, H.; Saliba, J.; Coureau, J.L.; Cointe, A.; Saiyouri, N. Long-Term Deformations and Mechanical Properties of Fine Recycled Aggregate Earth Concrete. *Appl. Sci.* **2022**, *12*, 11489. [CrossRef]
22. Yun, K.K.; Hossain, M.S.; Han, S.; Seunghak, C. Rheological, mechanical properties, and statistical significance analysis of shotcrete with various natural fibers and mixing ratios. *Case Stud. Constr. Mater.* **2022**, *16*, e00833. [CrossRef]
23. Rocha, J.H.A.; Galarza, F.P.; Chileno, N.G.C.; Rosas, M.H.; Peñaranda, S.P.; Diaz, L.L.; Abasto, R.P. Compressive Strength Assessment of Soil-Cement Blocks Incorporated with Waste Tire Steel Fiber. *Materials* **2022**, *15*, 1777. [CrossRef]
24. Venda Oliveira, P.; Correia, A.; Teles, J.; Custódio, D. Effect of fibre type on the compressive and tensile strength of a soft soil chemically stabilised. *Geosynth. Int.* **2016**, *23*, 171–182. [CrossRef]
25. Correia, A.A.; Oliveira, P.J.V.; Custódio, D.G. Effect of polypropylene fibres on the compressive and tensile strength of a soft soil, artificially stabilised with binders. *Geotext. Geomembranes* **2015**, *43*, 97–106. [CrossRef]
26. Sukontasukkul, P.; Jamsawang, P. Use of steel and polypropylene fibers to improve flexural performance of deep soil-cement column. *Constr. Build. Mater.* **2012**, *29*, 201–205. [CrossRef]
27. Tajdini, M.; Hajjalilue Bonab, M.; Golmohamadi, S. An experimental investigation on effect of adding natural and synthetic fibres on mechanical and behavioural parameters of soil-cement materials. *Int. J. Civ. Eng.* **2018**, *16*, 353–370. [CrossRef]

28. Ren, G.; Yao, B.; Ren, M.; Gao, X. Utilization of natural sisal fibers to manufacture eco-friendly ultra-high performance concrete with low autogenous shrinkage. *J. Clean. Prod.* **2022**, *332*, 130105. [[CrossRef](#)]
29. da Silva Segantini, A.A.; Wada, P.H. An evaluation of the composition of soil cement bricks with construction and demolition waste/Estudo de dosagem de tijolos de solo-cimento com adicao de residuos de construcao e demolicao. *Acta Sci. Technol.* **2011**, *33*, 179–184.
30. Kouta, N.; Saliba, J.; Saiyouri, N. Fracture behavior of flax fibers reinforced earth concrete. *Eng. Fract. Mech.* **2021**, *241*, 107378. [[CrossRef](#)]
31. Nascimento, E.S.S.; de Souza, P.C.; de Oliveira, H.A.; Júnior, C.M.M.; de Oliveira Almeida, V.G.; de Melo, F.M.C. Soil-cement brick with granite cutting residue reuse. *J. Clean. Prod.* **2021**, *321*, 129002. [[CrossRef](#)]
32. Eko, R.M.; Offa, E.D.; Ngatcha, T.Y.; Minsili, L.S. Potential of salvaged steel fibers for reinforcement of unfired earth blocks. *Constr. Build. Mater.* **2012**, *35*, 340–346.
33. Koutous, A.; Hilali, E. Reinforcing rammed earth with plant fibers: A case study. *Case Stud. Constr. Mater.* **2021**, *14*, e00514. [[CrossRef](#)]
34. Gong, Z.; Han, L.; An, Z.; Yang, L.; Ding, S.; Xiang, Y. Empowering smart buildings with self-sensing concrete for structural health monitoring. In Proceedings of the ACM SIGCOMM 2022 Conference, Renton, WA, USA, 4–6 April 2022; pp. 560–575.
35. Thompson, D.; Augarde, C.; Osorio, J.P. A review of current construction guidelines to inform the design of rammed earth houses in seismically active zones. *J. Build. Eng.* **2022**, *54*, 104666. [[CrossRef](#)]
36. Curto, A.; Lanzoni, L.; Tarantino, A.M.; Viviani, M. Shot-earth for sustainable constructions. *Constr. Build. Mater.* **2020**, *239*, 117775. [[CrossRef](#)]
37. Baccocchi, M.; Savino, V.; Lanzoni, L.; Tarantino, A.; Viviani, M. Multi-phase homogenization procedure for estimating the mechanical properties of shot-earth materials. *Compos. Struct.* **2022**, *295*, 115799. [[CrossRef](#)]
38. Bekzhanova, Z.; Memon, S.A.; Kim, J.R. Self-sensing cementitious composites: review and perspective. *Nanomaterials* **2021**, *11*, 2355. [[CrossRef](#)]
39. Azhari, F.; Banthia, N. Cement-based sensors with carbon fibers and carbon nanotubes for piezoresistive sensing. *Cem. Concr. Compos.* **2012**, *34*, 866–873. [[CrossRef](#)]
40. Taheri, S.; Georgaklis, J.; Ams, M.; Patabendigedara, S.; Belford, A.; Wu, S. Smart self-sensing concrete: the use of multiscale carbon fillers. *J. Mater. Sci.* **2022**, *57*, 2667–2682. [[CrossRef](#)]
41. Ramachandran, K.; Vijayan, P.; Murali, G.; Vatin, N.I. A Review on Principles, Theories and Materials for Self Sensing Concrete for Structural Applications. *Materials* **2022**, *15*, 3831. [[CrossRef](#)]
42. Qiu, L.; Dong, S.; Yu, X.; Han, B. Self-sensing ultra-high performance concrete for in-situ monitoring. *Sens. Actuators A Phys.* **2021**, *331*, 113049. [[CrossRef](#)]
43. Meoni, A.; D’Alessandro, A.; Cavalagli, N.; Gioffré, M.; Ubertini, F. Shaking table tests on a masonry building monitored using smart bricks: Damage detection and localization. *Earthq. Eng. Struct. Dyn.* **2019**, *48*, 910–928. [[CrossRef](#)]
44. Gautam, A.; Mo, Y.; Chen, Y.; Chen, J.; Joshi, B. Carbon nanofiber aggregate sensors for sustaining resilience of civil infrastructures to multi-hazards. *Adv. Civ. Eng. Technol.* **2019**, *3*, 263–269.
45. Castañeda-Saldarriaga, D.L.; Alvarez-Montoya, J.; Martínez-Tejada, V.; Sierra-Pérez, J. Toward structural health monitoring of civil structures based on self-sensing concrete nanocomposites: a validation in a reinforced-concrete beam. *Int. J. Concr. Struct. Mater.* **2021**, *15*, 1–18. [[CrossRef](#)]
46. Galao, O.; Baeza, F.J.; Zornoza, E.; Garcés, P. Carbon nanofiber cement sensors to detect strain and damage of concrete specimens under compression. *Nanomaterials* **2017**, *7*, 413. [[CrossRef](#)] [[PubMed](#)]
47. Chung, D. Self-sensing concrete: from resistance-based sensing to capacitance-based sensing. *Int. J. Smart Nano Mater.* **2021**, *12*, 1–19. [[CrossRef](#)]
48. Chung, D. A critical review of electrical-resistance-based self-sensing in conductive cement-based materials. *Carbon* **2023**, *203*, 311–325. [[CrossRef](#)]
49. Han, B.; Yu, X.; Ou, J. *Self-Sensing Concrete in Smart Structures*; Butterworth-Heinemann: Oxford, UK, 2014.
50. Han, B.; Yu, X.; Ou, J. Multifunctional and Smart Carbon Nanotube Reinforced Cement-Based Materials. In *Nanotechnology in Civil Infrastructure: A Paradigm Shift*; Gopalakrishnan, K., Birgisson, B., Taylor, P., Attoh-Okine, N.O., Eds.; Springer: Berlin/Heidelberg, Germany, 2011; pp. 1–47. [[CrossRef](#)]
51. Reddy, P.N.; Kavyateja, B.V.; Jindal, B.B. Structural health monitoring methods, dispersion of fibers, micro and macro structural properties, sensing, and mechanical properties of self-sensing concrete—A review. *Struct. Concr.* **2021**, *22*, 793–805. [[CrossRef](#)]
52. Konsta-Gdoutos, M.S.; Metaxa, Z.S.; Shah, S.P. Highly dispersed carbon nanotube reinforced cement based materials. *Cem. Concr. Res.* **2010**, *40*, 1052–1059. [[CrossRef](#)]
53. D’Alessandro, A.; Ubertini, F.; Materazzi, A.; Laflamme, S.; Cancelli, A.; Micheli, L. Carbon cement-based sensors for dynamic monitoring of structures. In Proceedings of the 2016 IEEE 16th International Conference on Environment and Electrical Engineering (EEEIC), Florence, Italy, 7–10 June 2016; pp. 1–4.
54. D’Alessandro, A.; Birgin, H.B.; Ubertini, F. Carbon Microfiber-Doped Smart Concrete Sensors for Strain Monitoring in Reinforced Concrete Structures: An Experimental Study at Various Scales. *Sensors* **2022**, *22*, 6083. [[CrossRef](#)]
55. Birgin, H.B.; Laflamme, S.; D’Alessandro, A.; Garcia-Macias, E.; Ubertini, F. A weigh-in-motion characterization algorithm for smart pavements based on conductive cementitious materials. *Sensors* **2020**, *20*, 659. [[CrossRef](#)]

56. Birgin, H.B.; D'Alessandro, A.; Laflamme, S.; Ubertini, F. Hybrid carbon microfibers-graphite fillers for piezoresistive cementitious composites. *Sensors* **2021**, *21*, 518. [[CrossRef](#)]
57. Meoni, A.; D'Alessandro, A.; Downey, A.; García-Macías, E.; Rallini, M.; Materazzi, A.L.; Torre, L.; Laflamme, S.; Castro-Triguero, R.; Ubertini, F. An experimental study on static and dynamic strain sensitivity of embeddable smart concrete sensors doped with carbon nanotubes for SHM of large structures. *Sensors* **2018**, *18*, 831. [[CrossRef](#)]

**Disclaimer/Publisher's Note:** The statements, opinions and data contained in all publications are solely those of the individual author(s) and contributor(s) and not of MDPI and/or the editor(s). MDPI and/or the editor(s) disclaim responsibility for any injury to people or property resulting from any ideas, methods, instructions or products referred to in the content.